Pacquelet et al., http://www.jcb.org/cgi/content/full/jcb.201503006/DC1

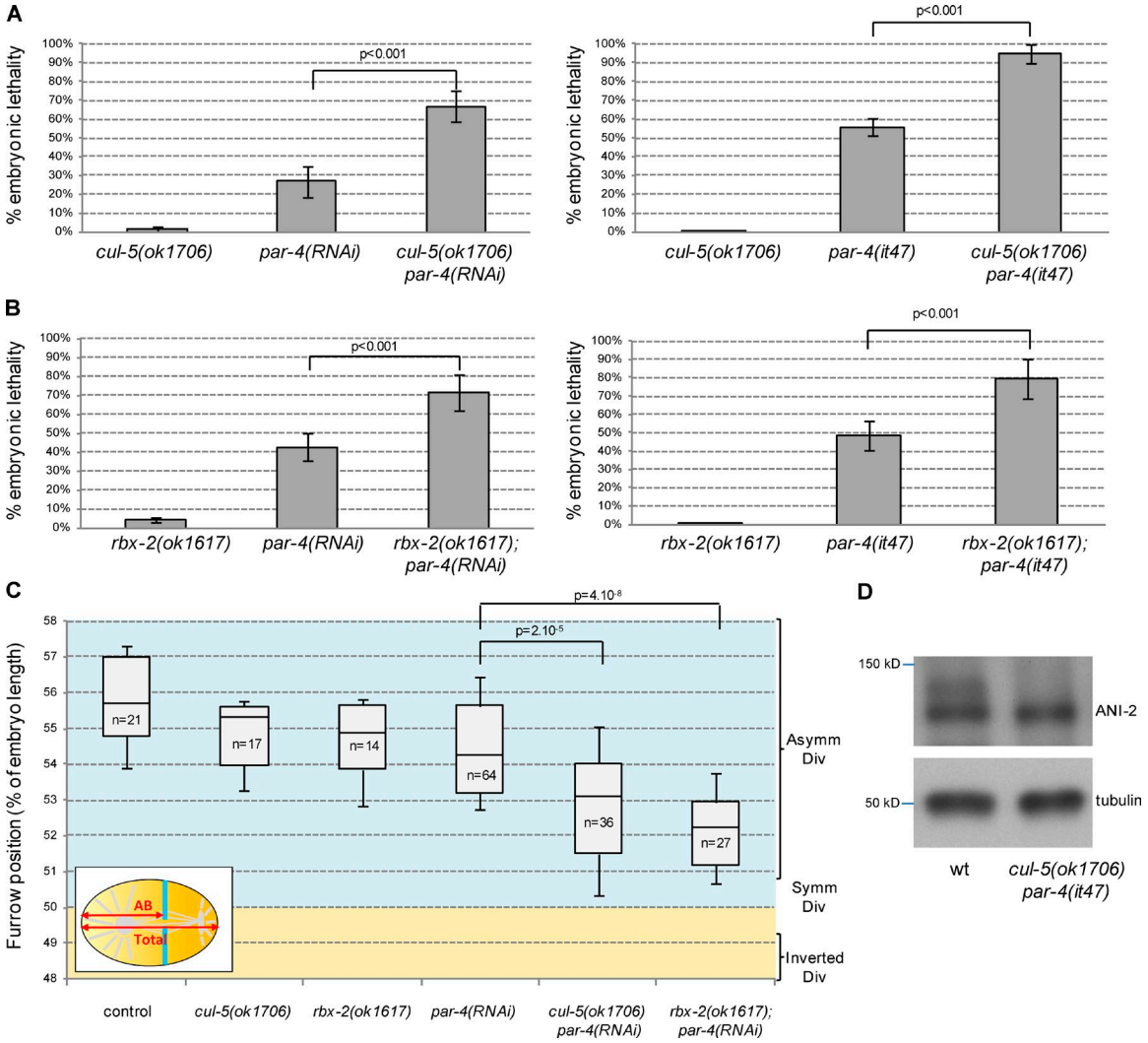

Figure S1. **CUL-5/RBX-2 and PAR-4 are synthetic lethal and regulate furrow positioning (related to Figs. 1 and 3).** (A and B) The loss of CUL-5 (A) and RBX-2 (B) increases *par-4(RNAi)* and *par-4(it47)* embryonic lethality. Error bars represent standard deviation. P-values from Wilcoxon test. (C) Quantification of furrow position in one-cell embryos of the indicated genotypes. The distance between the anterior pole and the furrow (AB size) was measured when the furrow spanned the entire embryo and is expressed as a percentage of embryo length (0% corresponds to the anterior pole and 100% to the posterior pole). P-values from Student's *t* test. (D) In *cul-5(ok1706) par-4(it47)* embryos, no change in ANI-2 total levels is detected by Western blot. Tubulin is used as a loading control.

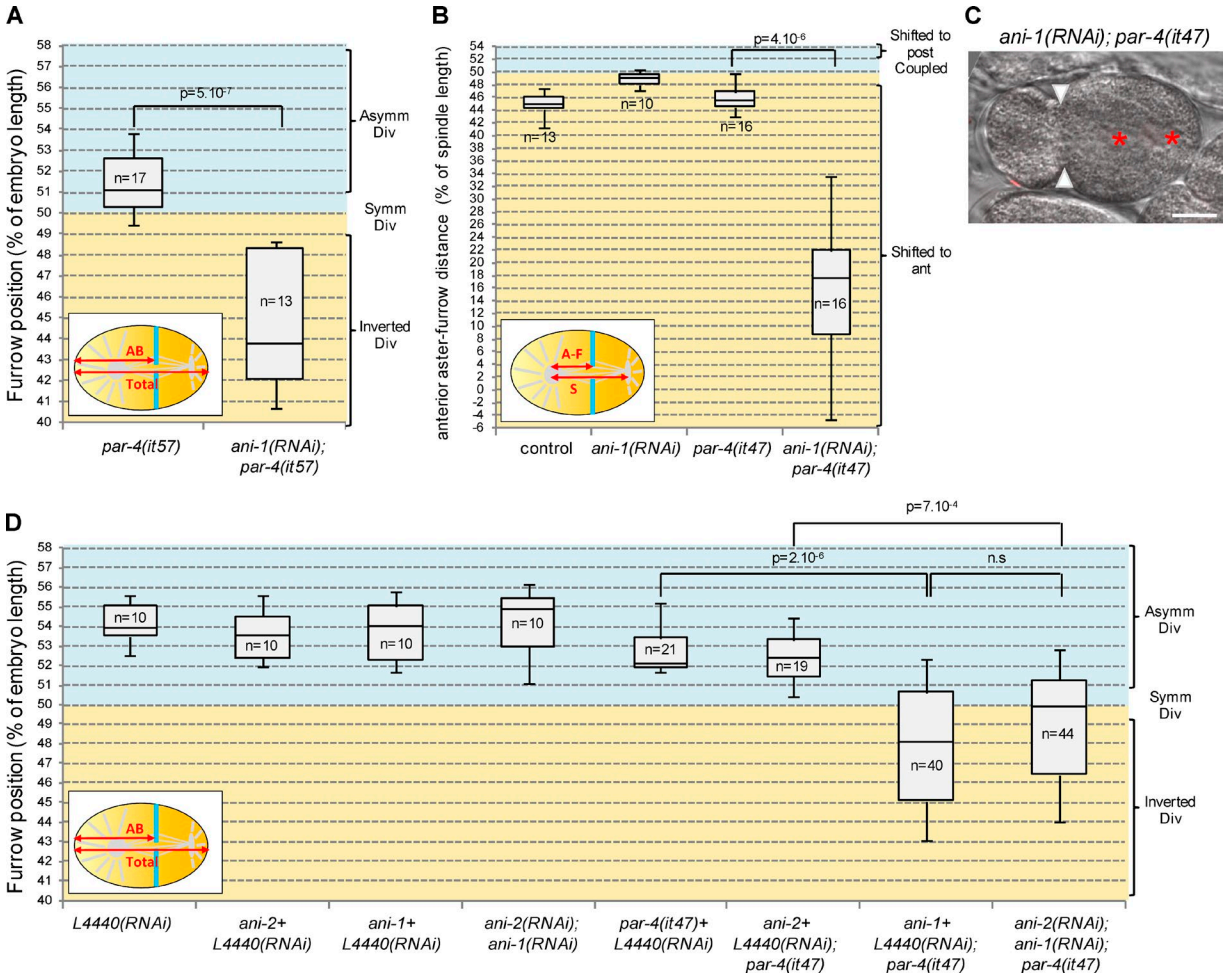

Figure S2. **Loss of PAR-4 and ANI-1 leads to strong furrow mispositioning (related to Fig. 4).** (A) *ani-1(RNAi); par-4(it57)* embryos show strong furrow mispositioning, similar to what was observed with the *par-4(it47)* allele (Fig. 4 B). The distance between the anterior pole and the furrow (AB size) was measured when the furrow reached its most anterior position. (B) Furrow and spindle positions are strongly uncoupled in *ani-1(RNAi); par-4(it47)* embryos grown at 25°C. The distance between anterior aster and furrow (A-F) was measured in dividing one-cell embryos when the furrow reached its most anterior position and is expressed as a percentage of spindle length (50% corresponds to the furrow position being coupled with spindle center, below 50% corresponds to a shift of the furrow toward the anterior, and above 50% corresponds to a shift toward the posterior). (C) Strong furrow mispositioning can lead to DNA segregation defects in *ani-1(RNAi); par-4(it47)* embryos. DIC image of an *ani-1(RNAi); par-4(it47)* embryo in which all DNA (asterisks) is inherited by the posterior cell. Arrowheads indicate furrow position. This embryo also expresses an mCherry::HIS-58 transgene to monitor DNA position. Four out of seven embryos showed this phenotype. Embryo is oriented with the anterior to the left. Bar, 10 µm. (D) Depletion of ANI-2 does not suppress furrow positioning defects in *ani-1(RNAi); par-4(it47)* embryos. The distance between the anterior pole and the furrow (AB size) was measured when the furrow reached its most anterior position. All p-values from Student's *t* test.

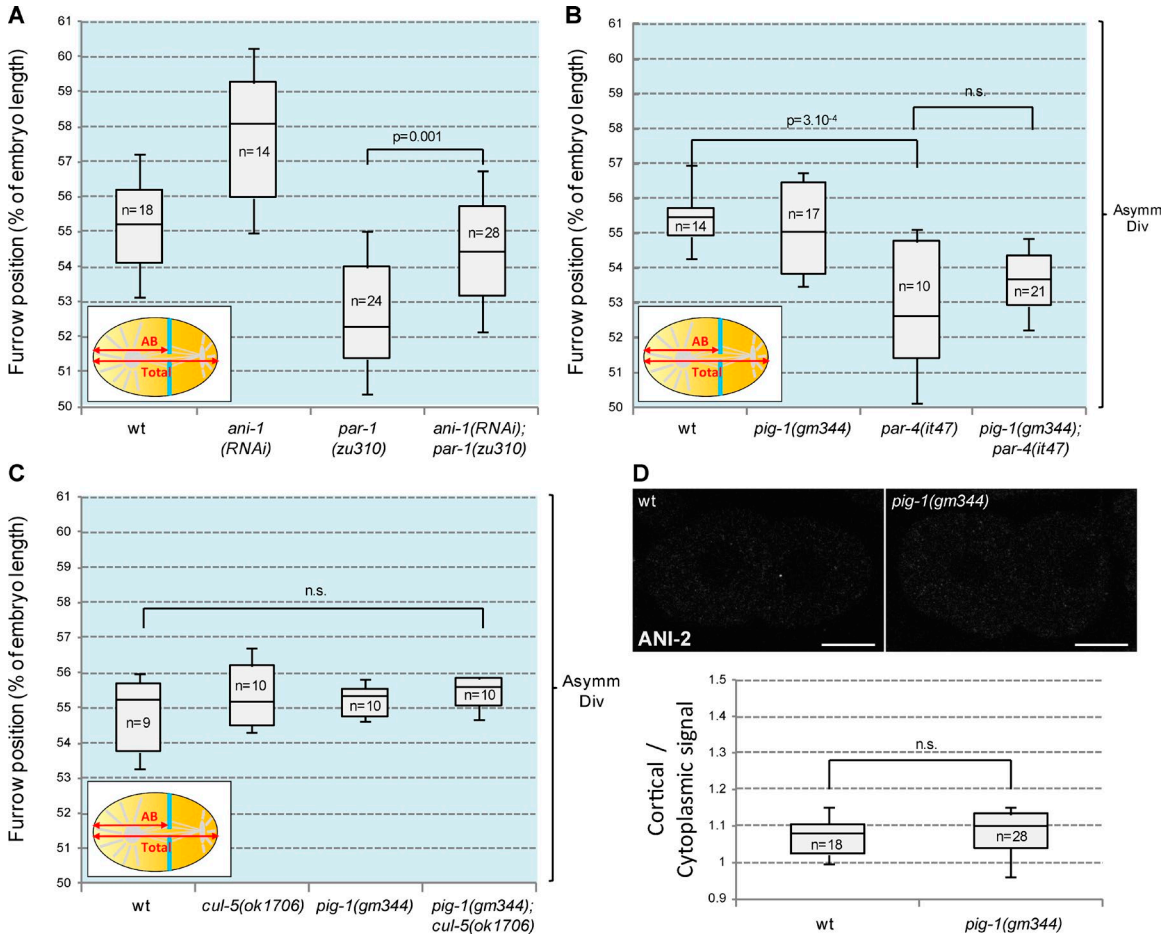

Figure S3. **Loss of PIG-1, but not PAR-1, and ANI-1 leads to strong furrow mispositioning (related to Fig. 5).** (A–C) Furrow position in *ani-1(RNAi); par-1(zu310)* (A), *pig-1(gm344);par-4(it47)* (B), and *pig-1(gm344); cul-5(ok1706)* (C) embryos. The distance between the anterior pole and the furrow (AB size) was measured when the furrow spanned the entire embryo. (D) ANI-2 immunostainings in *pig-1(gm344)* embryos. Confocal sections of two-cell embryos of the indicated genotypes stained with anti–ANI-2 antibody and quantification of ANI-2 accumulation at the cortex between AB and P1 (see Material and methods for details). Neither control nor *pig-1(gm344)* embryos show ANI-2 cortical accumulation. Bars, 10 µm. All p-values are from Student's *t* test.

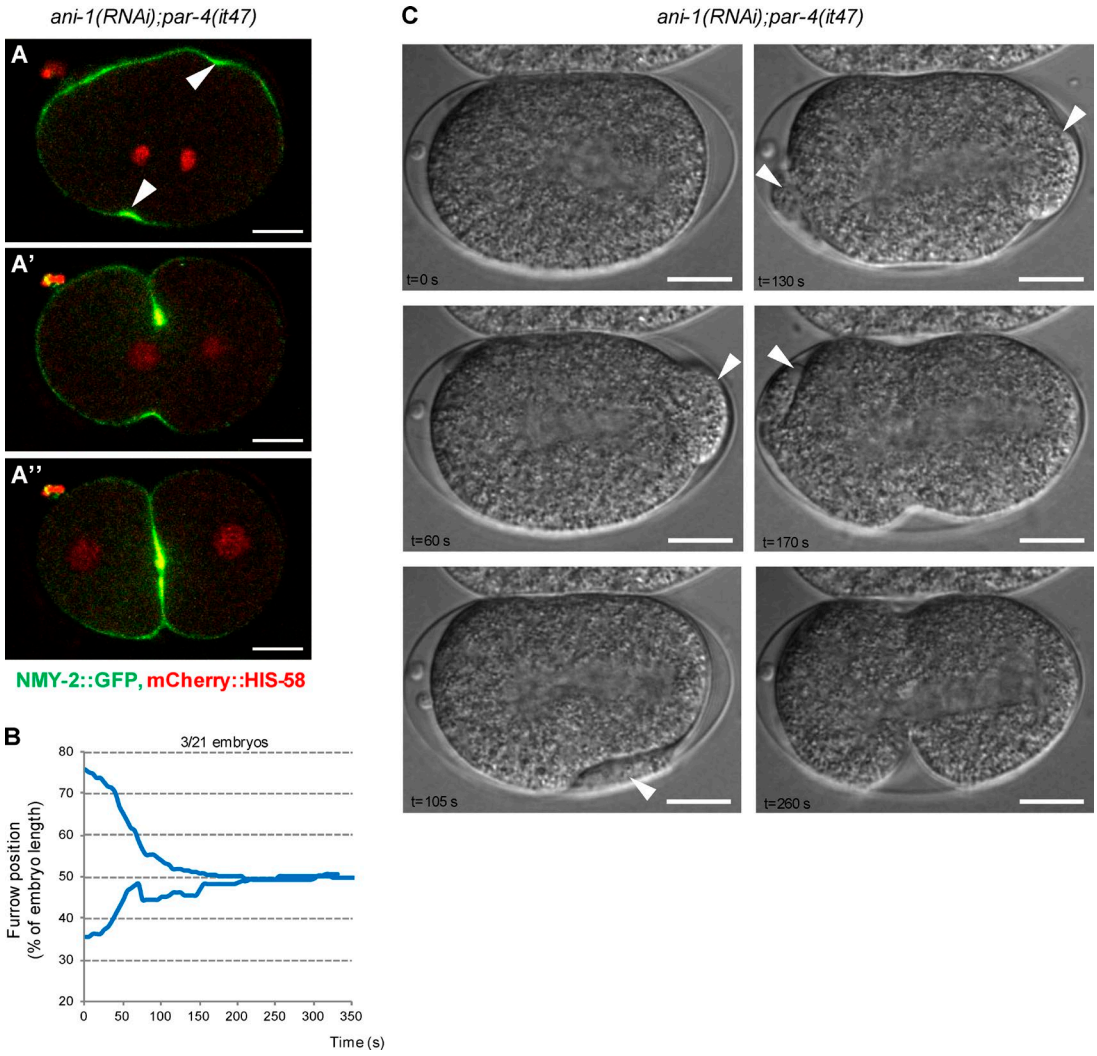

Figure S4. **Dynamics of furrow ingression and cortical deformations in *ani-1; par-4* embryos (related to Fig. 6 and Videos 6 and 9).** (A) In 3/21 embryos, one furrow tip started ingression very close to the posterior pole and another one very close to the anterior pole. Both furrow tips then moved simultaneously toward the center of the embryo. Furrow position during ingression is monitored with an NMY-2::GFP transgene (green). DNA is monitored with an mCherry::HIS-58 transgene (red). Images were taken at the onset of cytokinesis (A), during ingression (A′), and just after furrow closure (A″). Arrowheads indicate position of initial ingression on each side of the embryo. See also Video 6. (B) Graph representing the position of the furrow tips during ingression in the *ani-1(RNAi); par-4(it47)* embryo shown in A. Furrow tips were tracked from the initiation of ingression until furrow closure. Their positions are expressed as a percentage of embryo length (0% corresponds to the anterior pole and 100% to the posterior pole). Each track corresponds to the furrow tip position on one side of the embryo. (C) Still images of Video 9 showing cortical deformations in an *ani-1(RNAi); par-4(it47)* embryo (Video 9, left). Arrowheads point to the different areas of the cortex that are successively deformed. Bars, 10 µm.

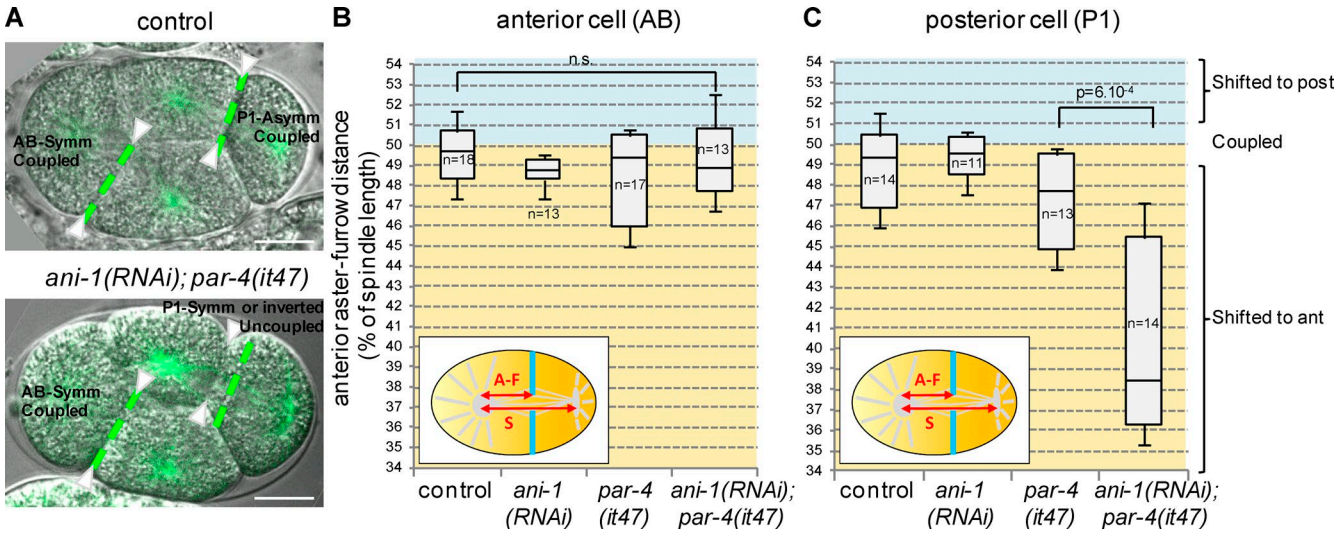

Figure S5. **PAR-4 and ANI-1 are required to coordinate furrow and spindle positions in asymmetrically dividing cells.** (A–C) In control two-cell embryos, the anterior AB cell divides symmetrically, whereas the posterior P1 cell is polarized and divides asymmetrically, giving rise to a smaller posterior cell. The mitotic spindle is centered in AB but displaced toward the posterior in P1. Spindle and furrow positions are coupled both in AB and P1. In *ani-1(RNAi); par-4(it47)* embryos, furrow position coincides with the spindle center in the anterior cell (A and B) but not in the posterior cell, with the furrow being displaced toward the anterior (A and C). Furrow position was not affected by inactivation of only PAR-4 or ANI-1 (B and C). Superposed confocal sections and DIC images (A) and quantifications of furrow/spindle coupling in the anterior (B) and posterior (C) cells of dividing two-cell embryos of the indicated genotypes (all strains also express an α-tubulin::YFP transgene [green]). Furrow position was measured when the furrow reached its most anterior position. Green dashed lines correspond to the spindle center and arrowheads correspond to furrow position. Bars, 10 μm. P-values from Student's *t* test.

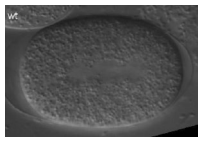

Video 1. **CUL-5/RBX-2 and PAR-4 regulate cytokinetic furrow position (related to Fig. 1 A).** DIC recordings of wild-type, *cul-5(ok1706)*, *rbx-2(ok1617)*, *par-4(it47)*, *cul-5(ok1706) par-4(it47)*, and *rbx-2(ok1617); par-4(it47)* dividing one-cell embryos. Images were recorded at 5-s intervals and movies are played at 5 frames per second. Embryos are oriented with anterior to the left.

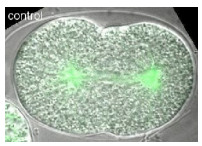

Video 2. **CUL-5 and PAR-4 regulate cytokinetic furrow position (related to Fig. 1 E).** Superposed DIC and confocal recordings of control, *cul-5(ok1706)*, *par-4(it47)*, and *cul-5(ok1706) par-4(it47)* dividing one-cell embryos (embryos also express α-tubulin::YFP [green]). Images were recorded at 5-s intervals and movies are played at 5 frames per second. Embryos are oriented with anterior to the left.

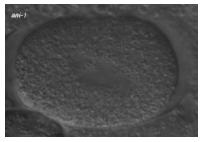

Video 3. **The loss of PAR-4 and ANI-1 leads to strong furrow mispositioning (related to Fig. 4 A).** DIC recordings of *ani-1(RNAi)* and *ani-1(RNAi); par-4(it47)* dividing one-cell embryos. Images were recorded at 5-s intervals and movies are played at 5 frames per second. Embryos are oriented with anterior to the left.

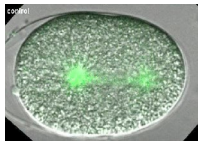

Video 4. **The loss of PAR-4 and ANI-1 leads to strong furrow mispositioning (related to Fig. 4 D).** Superposed DIC and confocal recordings of control, *ani-1(RNAi)*, *par-4(it47)*, and *ani-1(RNAi); par-4(it47)* dividing one-cell embryos (embryos also express α-tubulin::YFP [green]). Images were recorded at 5-s intervals and movies are played at 5 frames per second. Embryos are oriented with anterior to the left.

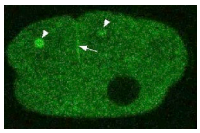

Video 5. **GFP::PIG-1 is recruited to the cortex during mitosis (related to Fig. 5).** Confocal and DIC recording of a dividing four-cell embryo expressing GFP::PIG-1 (green). Video starts after nuclear envelop has broken down in the two cells marked with asterisks. GFP::PIG-1 is localized in the cytoplasm and recruited to the cortex (arrow) and the centrosomes (arrowheads) during mitosis. Images were recorded at 20-s intervals and movie is played at 3 frames per second. Embryo is oriented with anterior to the left.

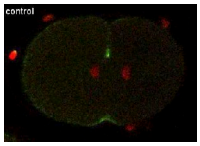

Video 6. **Dynamics of furrow ingression in *ani-1; par-4* embryos (related to Figs. 6 and S4).** Confocal recordings of control and *ani-1(RNAi); par-4(it47)* dividing one-cell embryos. The movie of the control embryo corresponds to the pictures shown in Fig. 6 A. The first (left) *ani-1; par-4* embryo corresponds to the pictures shown in Fig. 6 B and the second *ani-1; par-4* embryo corresponds to the pictures in Fig. S4 A. Embryos also express NMY-2::GFP (green) and mCherry::His-58 (red). Images were recorded at 5-s intervals and movies are played at 5 frames per second. Embryos are oriented with anterior to the left.

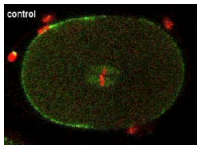

Video 7. **Dynamics of cortical myosin accumulation in control and *ani-1; par-4* one-cell embryos (related to Fig. 7 A).** Confocal recordings of control and *ani-1(RNAi); par-4(it47)* dividing one-cell embryos. Embryos also express NMY-2::GFP (green) and mCherry::His-58 (red). Images were recorded at 5-s intervals and movies are played at 5 frames per second. Embryos are oriented with anterior to the left.

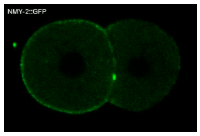

Video 8. **Dynamics of cortical myosin accumulation in control two-cell embryos.** Confocal recording of a dividing two-cell embryo expressing NMY-2::GFP (green). Images were recorded at 5-s intervals and movie is played at 5 frames per second. Embryo is oriented with anterior to the left.

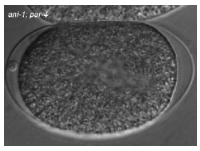

Video 9. **Cortical deformations and furrow position in *ani-1; par-4* and *nmy-2; ani-1; par-4* one-cell embryos (related to Figs. 8 A and S4 C).** DIC recordings of *ani-1(RNAi); par-4(it47)* and *nmy-2(ne1490); ani-1(RNAi); par-4(it47)* dividing one-cell embryos (embryos also express α-tubulin::YFP [not depicted]). Images were recorded at 5-s intervals and movies are played at 5 frames per second. Embryos are oriented with anterior to the left.

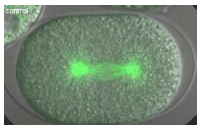

Video 10. **Hyperactivation of myosin in *rga-3/4(RNAi)* embryos leads to strong furrow mispositioning (related to Fig. 8 B).** Superposed DIC and confocal recordings of control and *rga-3/4(RNAi)* dividing one-cell embryos of the indicated genotypes (embryos also express α-tubulin::YFP [green]). Images were recorded at 5-s intervals and movies are played at 5 frames per second. Embryos are oriented with anterior to the left.

Table S1. **List of strains used for this study (related to experimental procedures)**

Name	Genotype	Type of mutation or construct	Origin
N2	wild-type strain	NA	*Caenorhabditis* Genetics Center (CGC)
KK184	*par-4(it47)*	*it47*: T to G substitution (bp 869 in cDNA)	D. Morton, Cornell University, Ithaca, NY, via CGC
KK300	*par-4(it57)*	*It57:* C to T substitution (bp 1165 in cDNA)	D. Morton, via CGC
FL41	*cul-5(ok1706)*	*ok1706:* 727 bp deletion (bp 1389–1853 in cDNA)	RB 1470 (Oklahoma Medical Research Foundation, via CGC) outcrossed 4×
FL75	*rbx-2(ok1617)*	*ok1617:* 759 bp deletion (bp 78–228 in cDNA)	RB 1420 (Oklahoma Medical Research Foundation, via CGC) outcrossed 5×
FL64	*cul-5(ok1706) par-4(it47)*		KK184 crossed with FL41
FL91	*rbx-2(ok1617); par-4(it47)*		KK184 crossed with FL75
TH65	*α-tubulin::YFP (unc-119(ed3); ddIs15 (α-tubulin::YFP)*	*ddIs15*: C47B2.3 genomic sequence, fused with YFP at C terminus	M. Srayko, Max Planck Institute of Molecular Cell Biology and Genetics, Dresden, Germany, via CGC
FL99	*α-tubulin::YFP; par-4(it47)*		TH65 crossed with KK184
FL142	*α-tubulin::YFP; cul-5(ok1706)*		TH65 crossed with FL41
FL98	*α-tubulin::YFP; cul-5(ok1706) par-4(it47)*		TH65 crossed with FL64
FL160	*mCherry::his-58(ltIs37); nmy-2::NMY-2::GFP(zuIs45)*	*ltIs37*: HIS-58 fused to mCherry at N terminus, under the control of pie-1 promoter *zuIs45*; NMY-2 fused to GFP at C terminus, under the control of *nmy-2* promoter	OD56 (J. Audhya, University of California, San Diego, CA, via CGC) crossed with JJ1473 (E. Munro, Fred Hutchinson Cancer Research Center, Seattle, WA, via CGC)
FL167	*mCherry::his-58; nmy-2::NMY-2::GFP par-4(it47)*		FL160 crossed with KK184
FL185	*α-tubulin::YFP nmy-2(ne1490)*	*ne1490:* G to A substitution (bp 2692 in cDNA)	TH65 crossed with WM180 (J. Liu, University of Massachusetts, Worcester, MA, via CGC)
FL190	*α-tubulin::YFP nmy-2(ne1490); par-4(it47)*		FL185 crossed with KK184
FL178	*pig-1(gm344)*	*gm344:* 524 bp deletion (removes bp 1–95 in cDNA)	NG4370 (G. Garriga, University of California, Berkeley, CA, via CGC) outcrossed to remove mec-4::GFP
FL200	*pig-1(gm344); par-4(it47)*		KK184 crossed with FL178
FL177	*pig-1(gm344); cul-5(ok1706)*		NG4370 (G. Garriga , via CGC) crossed with FL41, did not keep mec-4::GFP
FL184	*α-tubulin::YFP; pig-1(gm344)*		TH65 crossed with FL178
FL188	*pig-1(gm344); mCherry::his-58; nmy-2::NMY-2::GFP*		FL160 crossed with FL178
EU554	*zen-4(or153)*	*or153*: G to A substitutions at bp 1558 and 2202 of cDNA	D. Hamill, University of Oregon, Eugene, OR, via CGC
KK725	*nop-1(it142)*	*it142*: G to A substitution (bp 2088 in cDNA)	L. Rose, Cornell University, Ithaca, NY, via CGC
FL203	*GFP::PIG-1 (unc-119(ed3); pie-1::GFP::PIG-1(dfIs1))*	*dfIs1: pig-1* cDNA fused at the N terminus with GFP, under the control of *pie-1* promoter	DP38 bombarded with pID3.01B-*pig-1*

Table S2. **Experimental conditions used for this study (related to experimental procedures)**

Experiment	Plates used	Incubation temperature and time	Recording temperature
Fig. 1, A–C, E, and F; and Fig. S3, B and C	OP50	20°C for 24 h	20°C
Fig. 1 D	OP50	25°C for 24 h	Stainings
Fig. 2, A, B, and D–F	1 mM IPTG	20°C for 24–32 h	20°C
Fig. 2 C	OP50	25°C for 24 h	25°C
Fig. 3, A and B; Fig. 5, A–G; Fig. S1 D; and Fig. S3 D	OP50	20°C for 24 h	Stainings, blot
Fig. 3 C and Fig. S2 D	3 mM IPTG	20°C for 48 h	20°C
Fig. 4; Fig. 5, H–K; Fig. 6; Fig. 7, A and B; Fig. S2 A; Fig. S4, A and B; and Fig. S5	1 mM IPTG	20°C for 30–44 h	20°C
Fig. 7 C	1 mM IPTG	20°C for 72 h	Blot
Fig. 7 D	1 mM IPTG	20°C for 30–44 h	Stainings
Fig. 8, A and C	1 mM IPTG	20°C for 30–40 h	25°C
Fig.8, B and D	3 mM IPTG	25°C for 48 h	20°C
Fig. S1 C	3 mM IPTG	25°C for 48 h	25°C
Fig. S2, B and C; Fig. S3 A; and Fig. S4 C	1 mM IPTG	25°C for 30–40 h	25°C